

Interface and Friction Properties of Copper-embedded Polyethylene Terephthalate Filament

FOUED KHOFFI^{1*}, OMAR HARZALLAH² AND JEAN YVES DREAN²

¹Laboraty of Textile Engineering (LGTex), ISET Ksar-Hellal, University of Monastir, Tunisia

²Laboratoire de Physique et Mécanique Textiles (LPMT), ENSISA, Mulhouse, France

ABSTRACT

The aim of this study is to analyze the interfacial and the frictional properties of copper (Cu) reinforced polyethylene terephthalate (PET) filament. This Cu-Embedded PET filament will be used as an information transmitter. This filament was prepared by a co-extrusion process. Mechanical properties of these filaments have been quantified by tensile and pull-out analyses. It is shown that the mechanical properties of composite filament were improved by adding the copper filament (from 0.82 to 1.2 GPa). The results of the pull-out test revealed some adhesion between the copper and the PET despite the existence of a slippage of the copper filament in the PET matrix. Regarding the variation of the maximum pull-out load, according to the embedded length, a linearity relationship is observed. Therefore, it can be assumed that the interfacial shear stress is constant over the embedded length. Filaments surfaces have been analyzed after friction with Scanning Electron Microscope. Experimental results show a satisfying wear resistance of filaments, even if friction is able to induce some structural modifications of the polymer surface.

KEYWORDS: *Cu-Embedded PET filament, Interface, Friction, Wear, Pull-out test.*

INTRODUCTION

The textile industry has made considerable advances in the field of high value-added materials, mainly in the sectors of high-performance textiles and yarns. The use of new materials with specific properties and the

development of new structures and integration processes makes it possible to develop fabrics able to convey information while being mostly based on properties of electric conduction^[1-3]. Recently two different methods have been developed to synthesize conductive yarns and

to improve the mechanical properties. The first one is based on a melt spinning process. Different types of conducting fillers like metal powder, flake, carbon fibers and carbon black were used to make different conductive composites [4-5]. The second method is based on a coating process. A thin coating of conductive polymer from solutions onto the surface of plastics or textiles allows creating these conductive textiles structures [6-9]. Since polypyrrole coated polyester textiles have been developed by Milliken Research Corporation, many other research groups are active in this field [7]. In addition, polyaniline coated, or in-situ polymerized on non-woven fabric, nylon 6, cotton, polyester fabric and Nomex® fabric are recently reported [10-13].

Our research deals with a new approach for producing an information transmitter filament here after called “Cu-Embedded PET filament”. This method is based on the co-extrusion of a conductor filament with a polymer. The core is a copper filament and the sheath is a Poly(ethylene terephthalate) polymer (PET). This polymer can successfully be recycled, and copper offers good electrical properties [14]. During the co-extrusion step, the PET is melted and pumped through a furnace and then a spinneret. PET is particularly sensitive to the moisture during melt process at high temperature, and this is reflected on the rheological and mechanical properties [15-16]. There are three different degradation phenomena those can be complementary, thermal, mechanical and hydrolysis chains scission. Significant hydrolysis of PET is known to occur in wet or humid conditions at temperature above the melt temperature.

Hydrolysis chain scission is the fastest and the most dangerous degradation process [17-18].

The association matrix/fiber cannot be random [19]. It depends on the process of implementation, the chemical compatibility of materials to contact, the expected mechanical, thermal or electrical resistance, the quality of the interface reinforcement-matrix, etc. The fiber/matrix interface influences the properties of fiber-reinforced polymer composites. In general, fiber-reinforced composites should possess a good interfacial shear strength, τ_s , that is dependent upon the fiber surface properties and the mechanical properties of the fiber and the matrix. Several test methods have been developed for the evaluation of τ_s including fiber fragmentation [20], push-out [21] and the fiber pull-out test [22].

The PET is a polyester having a high melting point and the presence of aromatic ring and hydrophobic bands in its polymeric structure confers a mechanical strength and wear resistance in particular when it is used for applications subject to severe friction, e. g. during the weaving process. Bhimaraj et al., [23] showed that the properties of wear and friction strongly depend on the crystallinity of PET under quite specific conditions of moisture and temperature. These properties of friction can also depend on the orientation of the macromolecular polymer chains, thus the coefficient of friction can be decreased in the direction of orientation. If friction is perpendicular to the direction of the polymer chains this one will generate an abrasive action and that will cause the increase in the coefficient of friction. When PET is amorphous, wear is mainly of adhesive type, on the other hand it is produced by phenomena of tiredness for fibers with high

crystallinity. However, when it is subjected to fatigue, PET becomes very unstable and can be damaged much more quickly. This is explained by the fact that these instabilities of friction are related to an important difference of the properties in static and dynamic frictions^[24].

Our study is divided in two parts. The first part of the research is devoted to analyzing the tensile mechanical behavior of copper filament, PET and Cu-Embedded PET filament. This part is completed by the determination of the pull-out energy to characterize the quality of the copper/matrix interface. The second part is related to the evaluation of the wear behavior and the electrical conductivity of Cu-Embedded PET filament. The

morphological study of the composite filament surface obtained by scanning electron microscopy analysis enables us to characterize the structural changes of the polymeric material during friction events.

MATERIALS AND METHODS

Materials

In this study, three types of samples were investigated: a copper filament, a virgin PET and our produced Cu-Embedded PET filament. The copper reinforcement used is produced by Goodfellow (purity: 99.9 %) and has a diameter of $50 \pm 5 \mu\text{m}$ and a linear density of $20 \pm 0.81 \text{ Tex}$. PET (Rhodia, titanium dioxide-free) was used in pelletized form. The characteristics of this polymer are shown in Table 1.

TABLE 1. PET Characteristics

	$[\eta](\text{dL/g})$	$M_w(\text{g/mol})$	$T_f (^{\circ}\text{C})$	MFI (g/10min)	Linear density (Tex)
PET	0.74	42/100	253	20	21.35

$[\eta]$: Intrinsic Viscosity, M_w : molecular weight, T_f : melting temperature and MFI: Melt Flow Index at ambient temperature.

It should be pointed out that PET pellets have to be dried before the co-extrusion process. Otherwise the molecular weight will be considerably reduced due to hydrolysis of PET. The moisture content of PET should not exceed 0.005% by weight. So, the PET pellets were dried in vacuum at 120°C for 12 h in order to eliminate the residual moisture content.

A laboratory scale melt spinning unit (Filatech) used in this study is a standard device that has been modified. This spinning machine can produce simple filaments. To obtain Cu-

Embedded PET filament, we made the following modifications to the original machine: addition of a copper wire feed system, installation of a hollow piston, installation of a speed reducer (10% reduction) and addition of a filament guide device. This melt spinning machine was employed with the following configuration: 3-20 mm/min extruder speed, single-hole spinneret type, 1.5 mm spinneret dimension, a take up speed of 20 m/min, resident time of 7 min and extrusion temperature of 275°C . The extrudate is cooled in air then passed through a winding unit (Figure 1).

The drawing ratio ($\lambda \approx 200\times$) is calculated from the ratio of the winding roll speed on the delivery roll speed.

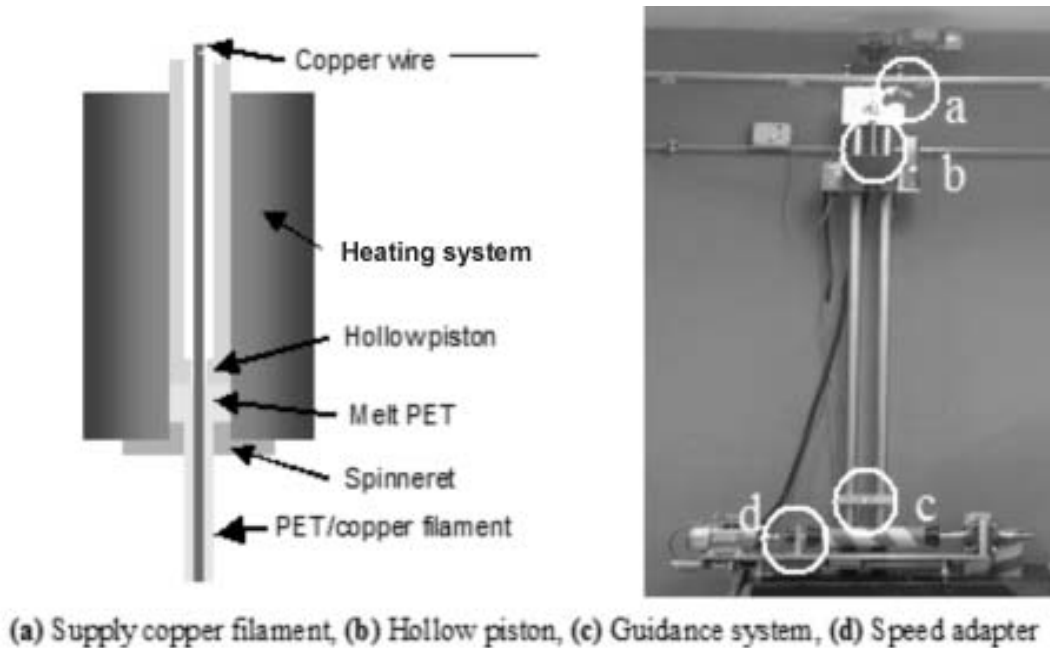


Fig. 1. Device for producing Cu-Embedded PET filament.

METHODS OF ANALYSIS

Mechanical Tensile and Pull-out Measurements

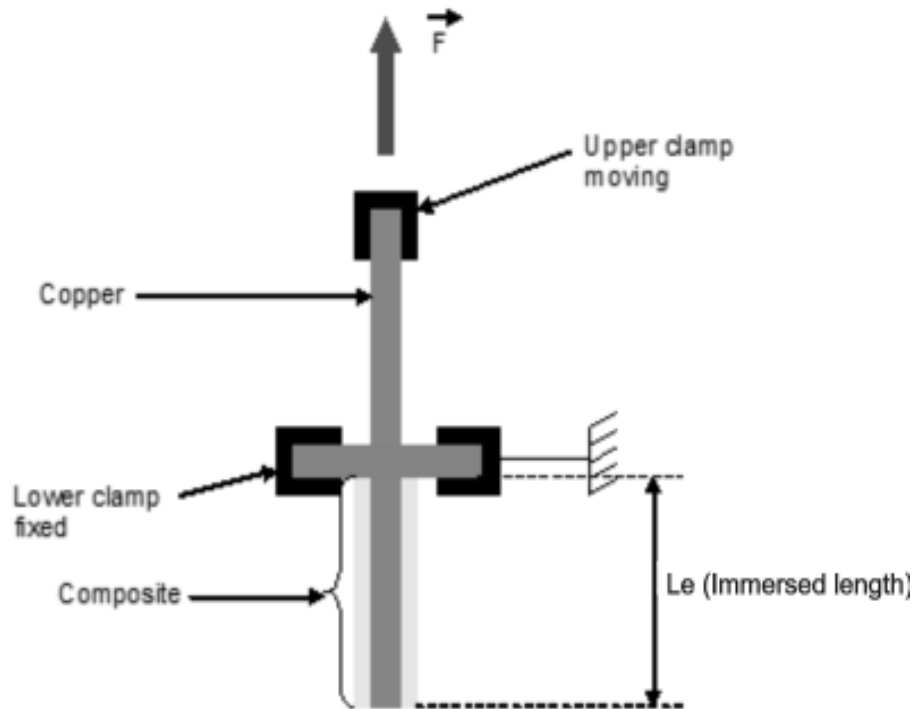
Mechanical tests were carried out using a dynamometer MTS/20. During tensile and pull-out test, the specimens were tested to failure at the crosshead speed of 10 mm/min under a pre-tension of 0.2 cN/tex^[25-26]. A high sensitive sensor of 10 N was used to obtain mechanical data. All tests were performed in a temperature-controlled room at 21 + 1°C and 65 + 2% relative humidity (RH)^[27].

In the pull-out experiment (Figure 2), the copper filament is embedded in the PET matrix (filament are produced by the spinning machine). A steadily increasing force is applied

using a dynamometer MTS/20 to the free end of the copper filament in order to pull it out the matrix. Load and displacement are recorded as the filament is pulled out until either pull-out occurs or the filament fractures.

Wear tests

Friction experiments are performed with a translation tribometer (Microtechnical Swiss Center). Measurements were carried out on the PET/copper filaments, obtained by melt spinning with a diameter of $235 \pm 5 \mu\text{m}$ and a linear density of $91.12 \pm 4.13 \text{ Tex}$. Filaments subjected to friction test (speed 100 mm min⁻¹ and normal load applied 6N) for 2 hours have been observed by using a Scanning Electron Microscopy (JEOL, JSM-IT100). This technique



Le: The immersed length of copper filament in PET matrix

Fig. 2. Illustration of the pull-out test using a dynamometer.

is allowed to determine geometrical characteristics of wear issue from friction between PET/copper filament and steel.

RESULTS AND DISCUSSION

Analysis of Tensile and Pull-out Tests

In order to analyze the mechanical performances of filaments, tensile and pull-out test were carried. In the first section, we studied the tensile mechanical behavior of initial copper, PET and Cu-Embedded PET filament. Thirty filaments were tested for each sample by using

a tensile testing machine MTS/20. Previous study conducted in our laboratory^[28] showed that the mechanical properties of composite filament were improved by adding the copper filament. The Cu-Embedded PET filament shows a ductile behavior (Figure 3) and the associated experimental modulus was verified by the mixture law^[29] from the associated modulus of PET (0.82 + 0.03 GPa) and copper (92.5 + 1.6 GPa) according to the following equation:

$$E_{th} = \phi_{PET} \cdot E_{PET} + \phi_{Cu} \cdot E_{Cu} \quad (1)$$

Where ϕ_{PET} and ϕ_{Cu} are respectively volume fractions of PET and copper in composite filament. E_{PET} and E_{Cu} are Young modulus for the associated materials.

According to equation 1, the theoretical modulus is $E_{th} = 4.67$ GPa. The experimental modulus was larger, at $E_{exp} = 1.2 \pm 0.1$ GPa. It can be observed that the load applied to the PET sheath ($E = 0.82$ GPa) was transmitted

to the copper core ($E = 92.5$ GPa). However, the difference between Young's modulus of composite (1.2 GPa) and copper filament (93 GPa) is due to the small section area of the copper filament compared to the composite. Figure 3(a) and (b) illustrate the cross section of the PET/copper composite filament. They also show that the copper filament seems to be greatly centered.

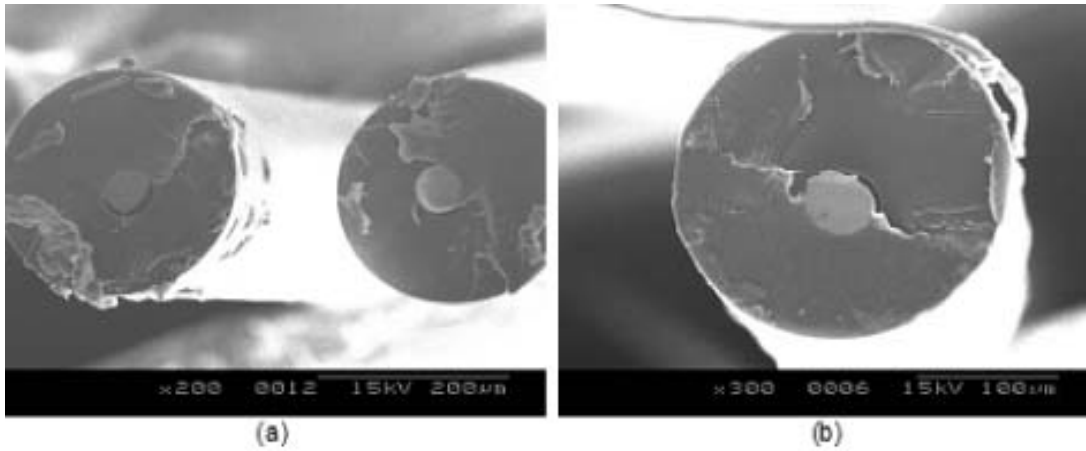


Fig. 3. Electron micro-graphs for the cross section of the Cu-Embedded PET filament by SEM.

Two types of curves were observed (Figure 4) in stress-strain graph for the pull-out experiments. In the first case (The immersed length of copper filament in PET matrix: $L_e = 4 - 6$ cm), the embedded length is very small compared to the free part of filament, the peaks that occurred after interfacial failure in the descending region of the force displacement curves may be attributed to the progressive extraction of the filament. The frictional pull-out loads are monitored until final failure. Fauvre^[30] has commonly observed this type of curve for weakly bonded interfaces.

In the second case ($L_e = 8-10$ cm), the embedded length is very close to the filament free length, the shape of the two curves resembles to the copper filament curve (Figure 4). It can, also, be noticed that for each test the rupture always occurs at the level of the copper filament. We can suppose that the stored energy within the system is not enough high to extract the filament after the initiation of interfacial failure and only the maximum pull-out force can be recorded.

It can be concluded that the shape of the force/displacement curve obtained from the pull-out

test depends on the intrinsic characteristics of the interface. It has been pointed out that there is a sudden release of strain energy stored in the free part of the fiber under tension where the interface fails. The elastic contraction may result in the full extraction of the filament from the matrix.

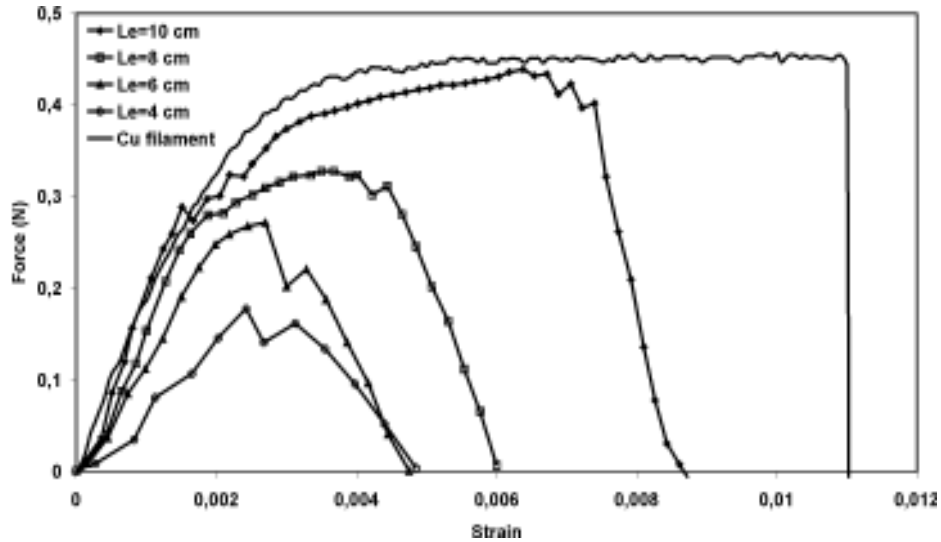


Fig. 4. Load/displacement curves for the Cu-Embedded PET filament pull-out test (with L_e : the embedded length of copper filament in PET matrix)

We are also interested in the variation of the maximum pull-out load, F_p^{max} (N), according to the embedded length, L_e (m). Figure 5 shows typical pull-out data, obtained using a tensile testing machine, for our PET/copper system with a variety of embedded lengths. A linearity relationship is observed. Therefore, it can be assumed that the interfacial shear stress is constant over the embedded length^[31].

The filament/matrix interface, τ_s (Pa), is calculated from:

$$\tau_s = \frac{F_p^{max}}{\pi d L_e} \quad (2)$$

Where d (m) is the filament diameter.

The determination of τ_s from the experimental data in this manner ignores stress concentrations and is therefore normally referred to as a mean apparent interfacial shear strength. Applying this approach to the data in Figure 5, we obtain $\tau_s \approx 0.0273 \text{ Mpa}$.

The results are in accordance with the previous theory of the linearity between the pull-out force and the embedded length^[32-35].

Wear Profile by Scanning Electron Microscopy (SEM)

Tribological tests were performed in order to evaluate the integration ability of composite filaments in textile fabrics, where it will be

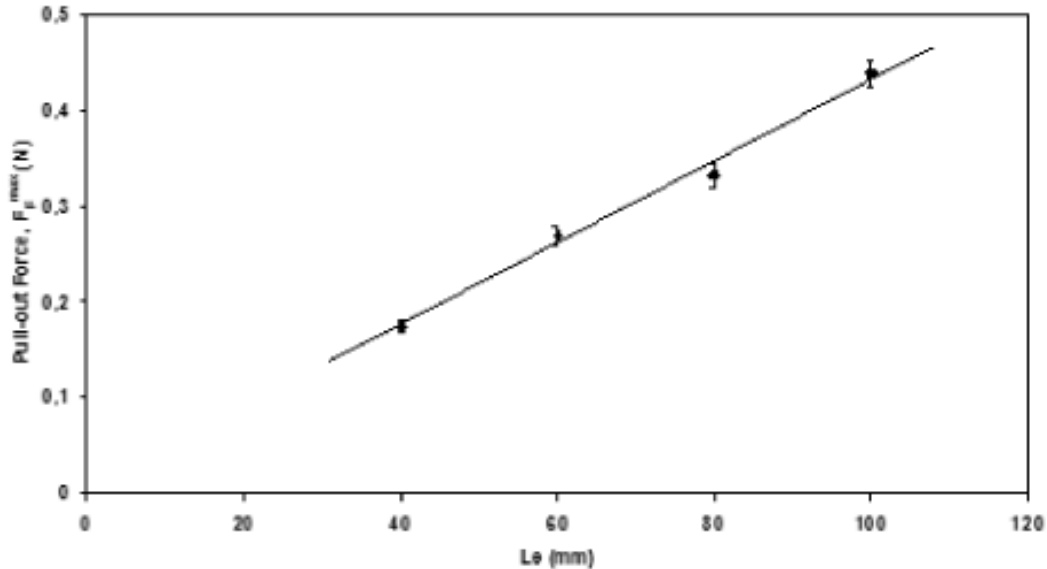


Fig. 5. Experimental data for the dependence of the pull-out force upon embedded length for the Copper/PET system investigated.

submitted to several stress. The results of static friction coefficient are presented in Table 2. The static friction coefficient (μ) between two solid surfaces, composite filament and steel in our case, is defined as the ratio of the tangential

force (FT) required to produce sliding divided by the normal force (FN) between the surfaces.

$$\mu = FT / FN \quad (3)$$

TABLE 2: Friction Coefficient at Constant Friction Speed 100 mm/min

Normal load Applied (N)	1	3	6	8
Friction coefficient (μ)	0.21	0.27	0.32	0.33

Following to friction tests, we observe an elliptical eroded area of 1.65 mm estimated length (Figure 6). We note the presence of crystals agglomerates localized on the edges of the worn surface, which illustrates the damage of the filament^[36]. It is known that at a temperature above the glass transition temperature of the polymer, cyclic oligomers

actively migrate from the inner regions to the eroded surface of the filament^[37-39]. Hence the polymer agglomerates (pieces of molten polymer) can be identified as oligomers^[40-41].

Electrical Conductivity Measurements

In this part, we measure the electrical conductivity of copper wire and PET matrix in

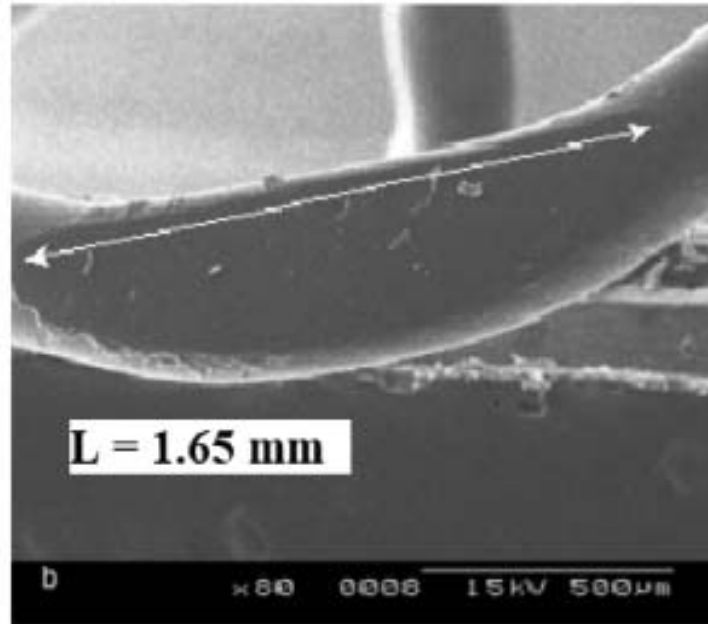


Fig. 6. Scanning electron micrograph of rubbed PET/copper filament. Load: 8 N, V: 100 mm/min, t: 10 min

Cu-Embedded PET filament. For this, we measured the electrical resistance of these filaments with an ohmmeter. Then, the electrical conductivity is calculated by the following formula:

$$\sigma = L / (S \cdot R) \quad (4)$$

With:

R : electrical resistance of the wire (Ω);

L : length of the filament (m);

S : cross-section of the filament (m^2).

The electrical conductivity measurement for the copper wire and PET matrix in the Cu-Embedded PET filament revealed the following values: $\sigma_{\text{copper}} = 27.2 \cdot 10^6$ Siemens/m and $\sigma_{\text{PET}} = 5.16 \cdot 10^{-3}$ Siemens/m. These results are in accordance with the previous study in literature [7,42-44].

However, the Cu-Embedded PET filament remains insulating at the outer surface confirming the protective role of the PET coating of the copper wire. These results are in contrast with the tribological tests where the wear caused on the Cu-Embedded PET filament remains produced only on the PET matrix.

CONCLUSION

The analysis of the results obtained from the tensile and pull-out tests show that the shape of the force/displacement curve is depended on the dynamics of the test and the intrinsic characteristics of the interface. It can be seen that the pull-out strain is lower in comparison with the tensile strain of copper filament. This revealed that during the pull-out test that there is a sudden release of strain energy stored in the free part of the fiber under tension where

the interface fails inducing a rupture in the free part of the filament. Indeed, the stored energy within the system is not enough to extract the filament from the matrix showing some adhesion between the copper and the PET.

The Cu-Embedded PET filaments that underwent periods of friction for three hours were observed by scanning electron microscopy (SEM). The observation of wear facies has determined that the copper filament has not been reached and that wear on these materials is caused by a warming of matter rather than by abrasion. According to these observations, the presence of oligomers is confirmed in the Cu-Embedded PET filament. This can explain the phenomenon of a slippage observed in the pull-out test.

This study highlights an acceptable quality of PET/Cu interface as well as a good wear behavior of the PET surface filament. These results show that the use of such filaments as material in weaving operation could be possible and interesting for technical uses.

References

1. J. Anand, S. Palaniappan and D. N. Sathyanarayana. (1998). *Prog. Polym. Sci.* 23(6): 993.
2. S. B. Gulas and H. M. Imre. (2020). *J. Fash. Technol. Text. Eng.* 8:4 198.
3. R. Kumar. (2020). *J. Polym. Mater.*, 37(3):131.
4. X. Juan, M. Menghe and J. Yongtang. (2020). *Autex Res. J.* 20(1): 63.
5. X. Li, T. Hua, B. Xu. (2017). *Carbon* 118: 686.
6. C. Gunesogluab, S. Gunesogluab, S. Weic and Z. Guoa. (2011). *J. Text. Inst.* 102 (5): 434.
7. Z. Li, G. Luo, F. Wei and Y. Huang. (2006). *Compos. Sci. Technol.* 66(7): 1022.
8. L. Allison, S. Hoxie, T. L. Andrew. (2017). *Chem Commun* 53: 7182.
9. M. K. Marichelvam and K. Kandakodeeswaran, (2017). *J. Polym Mater*, 34(4): 733.
10. H. H. Kuhun and A.D. Child, Handbook of Conductive Polymer, 2nd ed., Terje A. Skotheim, Ronald L. Elsenbaumer, John R. Reynolds (Eds). (1998). Marcel Dekker: New York, Ch 35.
11. S. H. Kim, J.H. Seong and K.W. Oh. (2002). *J. Appl. Polym. Sci.* 83(10): 2245.
12. K.W. Oh, S.H. Kim and E.A Kim. (2001). *J. Appl. Polym. Sci.* 81(3): 684.
13. B. Zhang, T. Xue, J. Meng and H. Li. (2015). *J. Text. Inst.* 106 (3): 253.
14. L. Lu, Y. Shen, X. Chen, L. Qian and K. Lu. (2004). *Science* 304(5669): 422.
15. A. Elamri, A. Lallam, O. Harzallah and L. Bencheikh. (2007). *J. Mater Sci.* 42(19): 8271.
16. J. Bitenieks, R.M. Merijs, J. Zicans, K. Buks. (2020). *Int. J. Mater Sci.* 1.
17. W. McMahon, H.A. Birdsall, G.R Johnson and C.T Camilli. (1959). *J. Chem. Eng. Data* 4: 57.
18. S. Sawada, K. Kamiyama, S. Ohgushi and K. Yabuki. (1991). *J. Appl. Polym. Sci.* 42(4): 1041.
19. M. Reyne. (1995). *Technologie des composites*, 2e ed. Hermès : Paris.
20. M. R. Piggott, In interfacial Phenomena in composite Materials, I. Verpoest I. & F.R. Jones (Eds). (1991). Butterworth Heinemann: Oxford, UK, ch. 2.
21. J. F. Mandell, J. Chen and F. J. McGrary. (1980). Res. Rep. R80-1, Massachusetts Institute of Technology, School of Engineering, Cambridge, MA, p.8.
22. L.J. Broutman. (1969). American Society for Testing and Materials. Philadelphia, PA, p27.
23. P. Bhimaraj, D.L. Burris, J. Action, W.G. Sawyer, C.G. Toney, R.W. Siegel and L.S. Schadler. (2005). *Wear*, 258(9): 1437.

24. P. Samyn, J. Quintelier, W. Ost, P. De Baets and G. Schoukens. (2005). *Polym. Test.* 24(5): 588.
25. AFNOR, Méthodes de Détermination de la Force de Rupture et de l'Allongement de Rupture d'un Fil (NFG 07-003). (1998). Recueil de Normes Françaises, 5ème éd. : Paris, ch 3.
26. D. Aprialdi, S. Lambert, O. J. Erizal and M. Widyarti. (2014). *Civ. Eng. Dimens.*16(2): 61.
27. ASTM, Standard Practice for Conditioning Textiles for Testing (D-1776-90). (1997). *American Society for Testing and Materials: Philadelphia, PA*, p483.
28. F. Khoffi, N. khenoussi, O. Harzallah and J. Y. Drean. (2011). *Phys. Procedia* 21: 240.
29. Gay D. (2005). *Matériaux composites*, 5e ed. Hermès: Paris.
30. K. P. Fauvre and M.C. Merienne. (1981). *Int. J. Adhes. Adhes.*, 1(6): 311.
31. Z. F. Li and T. Grubb. (1994). *J. Mater. Sci.* 29: 189.
32. P. Lawrence P. (1972). *J. Mater. Sci.* 7: 1.
33. A. Takaku and R.G. Arridge. (1973) *J. Phys. D: Appl. Phys.*, 6: 2038.
34. G. Jakub, P. Jerzy. (2019). MATEC Web of Conferences, 252:08001.
35. H. R. Pakravan, M. Jamshidi and M. Latifi. (2013). *J. Text. Inst.* 104(10): 1056.
36. J.W. Hearse, B. Lamas and W.D. Cooke. (1998). The textile institute, 2nd ed., England.
37. W. Chaouch, F. Dieval, D. Le Nouen, A. Defoin, N. Chakfe and B. Durand. (2009). *J. Appl. Polym. Sci.* 113(5): 2813.
38. A. Perovic. (1985). *J. Mater. Sci.* 20(4): 1370.
39. S. P. Rwei and S. K. Ni. (2004). *Text. Res. J.* 74(7): 581.
40. K. Nagel, L. Kaßner, A. Seifert, R.E. Gruetzner, G. Coxb and S. Spange. (2018). *R. Soc. Chem.* 8: 14713.
41. J. Scheirs, Ed. (2000). John Wiley & Sons: England, p.618.
42. A. Lund, Y. Wu, B. Fenech?Salerno, F. Torrisi, T. B. Carmichael and C. Müller. (2021). *MRS Bulletin* 46: p491.
43. W. Eom, H. Shin, R. B. Ambade, S. H. Lee, K. H. Lee, D. J. Kang, T. H. Han. (2020). *Nat. Commun.* 11: 2825.
44. A. Lund, N. M. Van Der Velden, N. K. Persson, M. M. Hamedi and C. Müller. (2018). *Mater. Sci. Eng. R.* 126: 1.

Received: 08-01-2023

Accepted: 11-06-2023